

Electronic Supporting Information

Gecko toe pads inspired in-situ switchable superhydrophobic shape memory adhesive film

*Yongzhen Wang,^a Hua Lai,^a Zhongjun Cheng,^{*bd} Haiyang Zhang,^a Enshuang Zhang,^c Tong Lv,^c Yuyan Liu,^{*a} and Lei Jiang^d*

^aMIT Key Laboratory of Critical Materials Technology for New Energy Conversion and Storage, School of Chemistry and Chemical Engineering, Harbin Institute of Technology, Harbin 150001, P. R. China

^bAcademy of Fundamental and Interdisciplinary Sciences, Harbin Institute of Technology, Harbin 150090, P. R. China

^cAerospace Institute of Advanced Materials & Processing Technology, Beijing 100074, China

^dCAS Key Laboratory of Bio-inspired Materials and Interfacial Science, Technical Institute of Physics and Chemistry, Chinese Academy of Science, Beijing, 100190, P. R. China

Detailed information for the fabrication of the film:

Materials. The bacterial cellulose was purchased from Hainan Yida food industry *Co., Ltd.* The 88T90 (Mn = 37.6 kDa), a thermoplastic polyester polyurethane with a Shore hardness of about 90A and a density of about $1.22 \text{ g}\cdot\text{cm}^{-3}$ was supplied by ChinaSound Industrial Ltd. PDMS Sylgard 184 was purchased from Dow Corning, USA. Trichloro (1H, 1H, 2H, 2H-perfluorooctyl) silane was purchased from Sigma. Dimethylformamide (DMF) was purchased from Xilong Scientific Co., Ltd. Distilled water ($>1.82 \text{ M}\Omega \text{ cm}$) from the Milli-Q system was used.

Fabrication of CNF. The CNF were prepared by sulfuric acid hydrolysis of bacterial cellulose chips as previously described.¹ Briefly, the bacterial cellulose chips were first washed by pure water and dried overnight at 80°C . The obtained dry bacterial cellulose chips (5g) were then dispersed in 64% sulfuric acid (100 mL) at 55°C for about 2 h with a stirring rate of about 500-800 rpm. The reaction was terminated by diluting the solution with a 10-fold amount of deionized water. The resulting solution was further washed with a centrifuge at 10000 rpm for about 5 min. After dialysis (5 days) and lyophilisation (3 days), the purified CNF were collected.

Fabrication of PU-CNF. The PU-CNF layer was prepared by solvents casting process. As shown in Fig. S1a and S1b, the CNF and PU particles were firstly dispersed in DMF with the concentration of about $10 \text{ g}\cdot\text{L}^{-1}$ and $50 \text{ g}\cdot\text{L}^{-1}$, respectively. After that, the 10 mL CNF-DMF dispersion was slowly dropped into 5 mL PU-DMF solution under stirring to obtain a homogeneous mixture (Fig. S1c). Then the mixture was transferred to a Teflon mold and dried at 75°C for about 24 h (Fig. S1d).

Fabrication of s-PU film. The pillar structured superhydrophobic s-PU layer was prepared by replica-molding procedure (Fig. S1e-h). Briefly, the pillar structured silicon template was

firstly prepared by photolithography process that has been reported by several papers (Fig. S1e).² After that, the PDMS precursors were poured over the FAS (heptadecafluorodecyltrimethoxysilane) modified silicon substrate. After degassing for about 15 min under vacuum, the prepolymer mixture was cured at 70°C for 4 h, and then the PDMS mold can be obtained after peeling off carefully from the silicon substrate (Fig. S1f-S1g). Finally, the PU-DMF solution with a concentration of about 10 g·L⁻¹ was poured onto PDMS mold and baked at 75°C for about 5 h to obtain the s-PU layer (Fig. S1h).

Fabrication of s-PU/PU-CNF film. In order to obtain s-PU/PU-CNF film, a drop of PU-DMF solution (10 g·L⁻¹) was dropped onto the backside of s-PU thin layer (herein, the s-PU was still in the PDMS mold) and then the PU-CNF film was covered quickly onto the s-PU film (Fig. S1i). After thorough evaporation of DMF, two layers would stick together tightly (Fig. S1j). Finally, the film was obtained after carefully peeling from PDMS mold (Fig. S1k). Herein, in order to obtain the low adhesive curved shape, the film was coiled around a glass rod with the s-PU surface outside and further heated at 85°C for about 5 h (Fig. S1l).

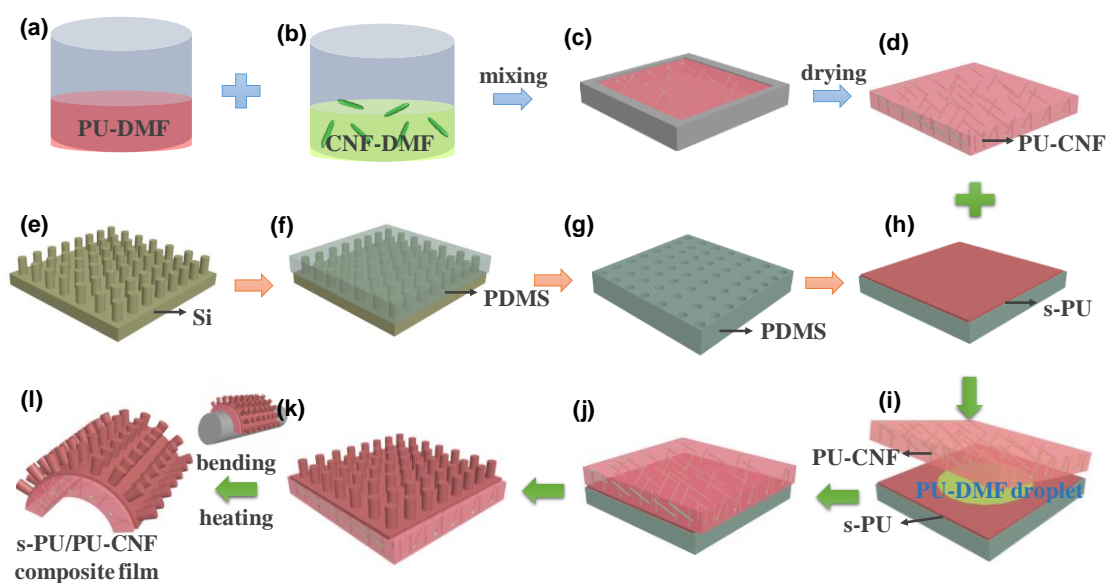


Fig. S1 Schematic illustration of fabrication process of the film.

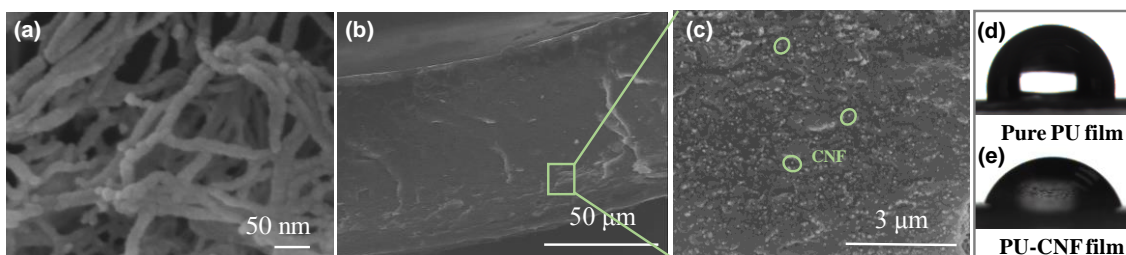


Fig. S2 (a) SEM image of CNF obtained by sulfuric acid hydrolysis. (b) and (c) are cross-sectional SEM images of PU-CNF substrate with low and high magnifications, respectively. (d, e) Shape of a water droplet (about 3 μ L) on the pure PU surface and the PU-CNF substrate, and corresponding water contact angles are about 97° and 69°, respectively. The SEM images tell us that nanoscale CNF can be dispersed uniformly into the PU, which can increase the hydrophilicity of the material.

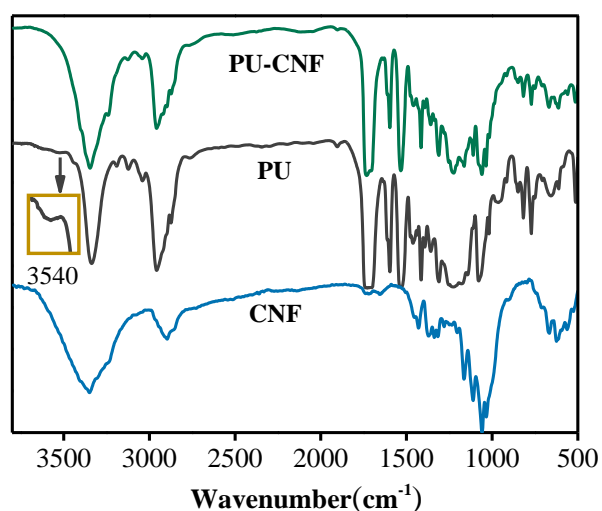


Fig. S3 The FTIR spectra of PU, CNF and PU-CNF film.

From Fig. S3, it can be seen that in the pure PU spectrum, the strong peak centered at about 3335 cm⁻¹ is assigned to the stretching vibration of N-H, the O-H adsorption peak at 3540 cm⁻¹ is very weak, indicating that in pure PU, the amount of O-H is very small, and thus

the pure PU shows hydrophobicity (Fig. S2d). In both CNF and PU-CNF, the strong and wide peaks in the range of 3200-3500 cm^{-1} and centered at 3350 cm^{-1} that are assigned to the stretching vibration of O-H can be observed, indicating that the O-H in PU-CNF composite is mainly from CNF. Meanwhile, because the amount of O-H is increased apparently after addition of CNF, the PU-CNF composite becomes hydrophilic (Fig. S2e).

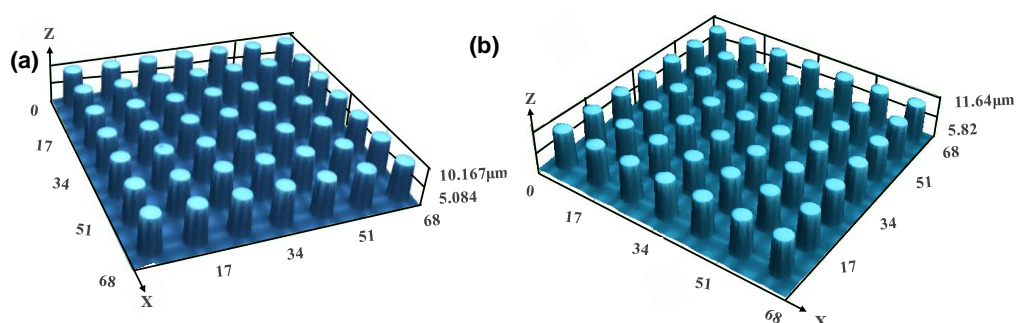


Fig. S4 (a) The 3D confocal microscopy images of Si template used for the fabrication of s-PU. (b) The 3D confocal microscopy images of the obtained s-PU. These results demonstrate that the used method can successfully replicate the targeted micropillars.

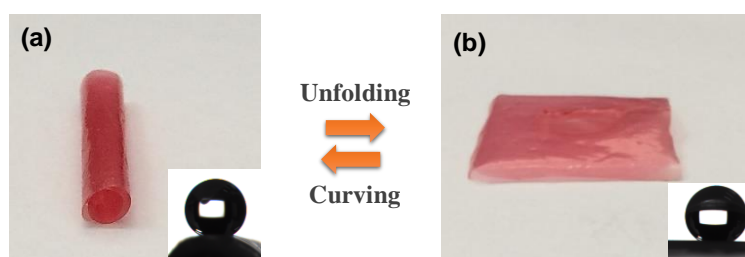


Fig. S5 The photos of the obtained film at curved shape (a) and unfolded shape (b), respectively. Insets are shapes of a water droplet on the surface corresponding to different states, indicating that the film shows the superhydrophobicity in both the two conditions.

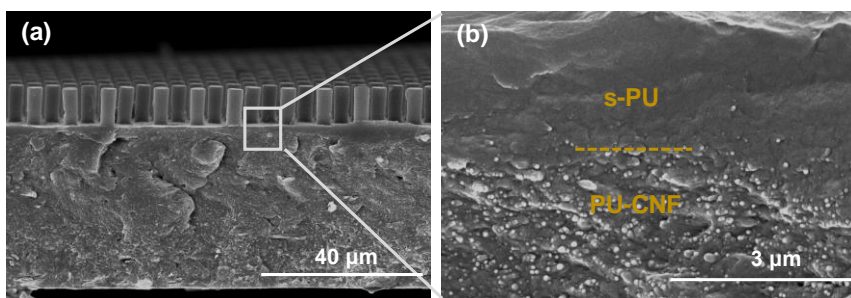


Fig. S6 Cross-sectional SEM images of the film after 50 times unfolding-curving shape memory cycles with low and high magnifications, respectively. It can be seen that after 50 times shape variations, the two layers (s-PU layer and PU-CNF layer) still stick together without obvious gaps, demonstrating a good fatigue durability.

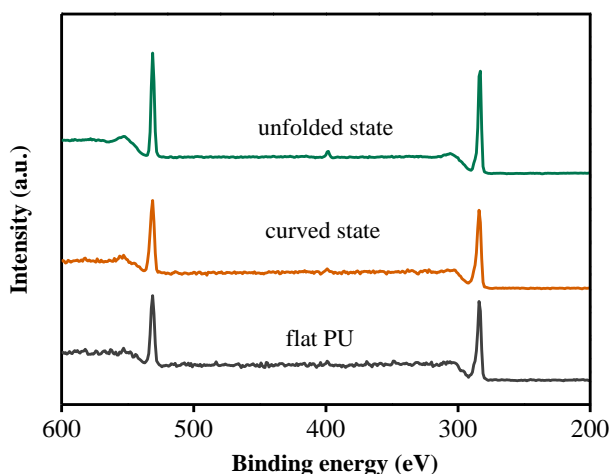


Fig. S7 The XPS spectra of flat PU surface and the s-PU surface of the obtained film at curved and unfolded states, respectively.

Table. S1 The element composition of flat PU and s-PU surface of the film including curved and unfolded states.

element	C	N	O
flat PU	73.67	3.56	22.76
film with curved shape	69.35	5.04	25.62
film with unfolded shape	71.12	2.62	26.25

From the Fig. S7 and Table S1, it can be seen that the s-PU surface of the as-prepared film at different states has the similar surface chemical composition with the flat PU, which can further confirm that the surface adhesion variation of the film is ascribed to the variation of surface microstructure.

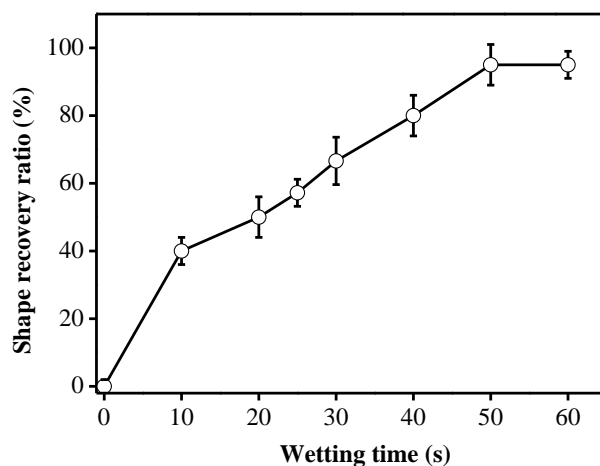


Fig. S8 The change of shape recovery ratio with the increase of wetting time. It can be seen that as the wetting time of the PU-CNF substrate is increased, the shape recovery ratio is increased, and when the wetting time is higher than 50 s, the film would get its maximal shape recovery ratio.

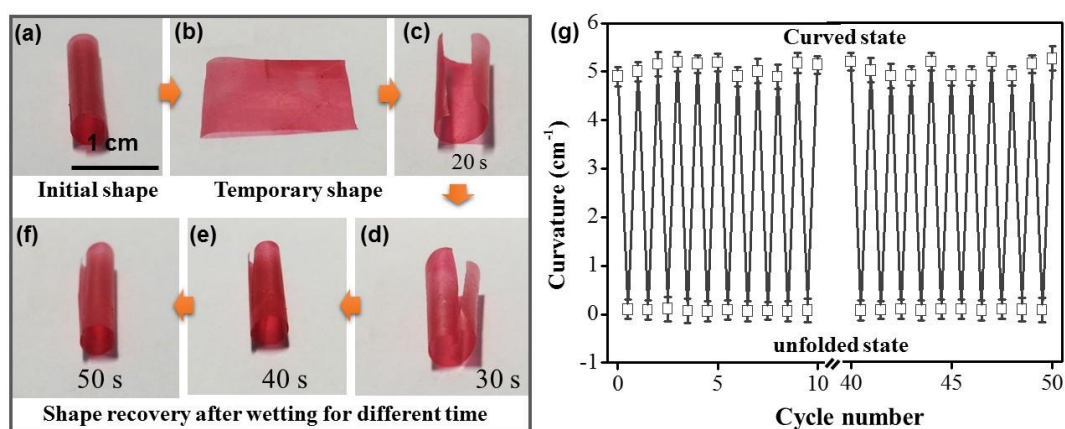


Fig. S9 The shape memory process (a-f) and shape memory cycle performance (g) of PU-CNF substrate (thickness of about 40 μm). From these figures, one can find that the PU-CNF substrate has good and stable shape memory property, which can keep the

responsivity even after 50 cycles shape variation. It can be seen that when the thickness of the shape memory PU-CNF film is similar, the integration of a thin s-PU film has no apparent effect on the shape memory ability of the film (Fig. 2a-f). The red color of the film was due to the presence of Sudan red for better observation since the pure PU-CNF film is transparent.

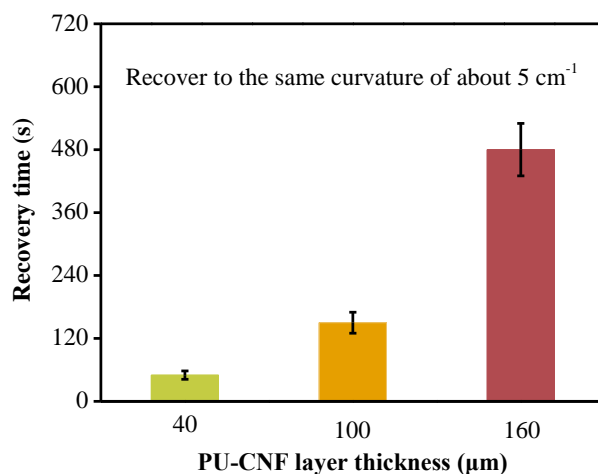


Fig. S10 The shape recovery velocity of films with different PU-CNF substrate layer thickness. It can be seen that with increasing the thickness of the PU-CNF substrate, the shape recovery velocity is decreased. As the thickness was further decreased, we found that the film has a poor mechanical strength, which cannot keep the unfolded state. In this work, to obtain the high adhesive unfolded shape and relatively fast recovery velocity, the thickness of the PU-CNF substrate was fixed at about 40 μm .

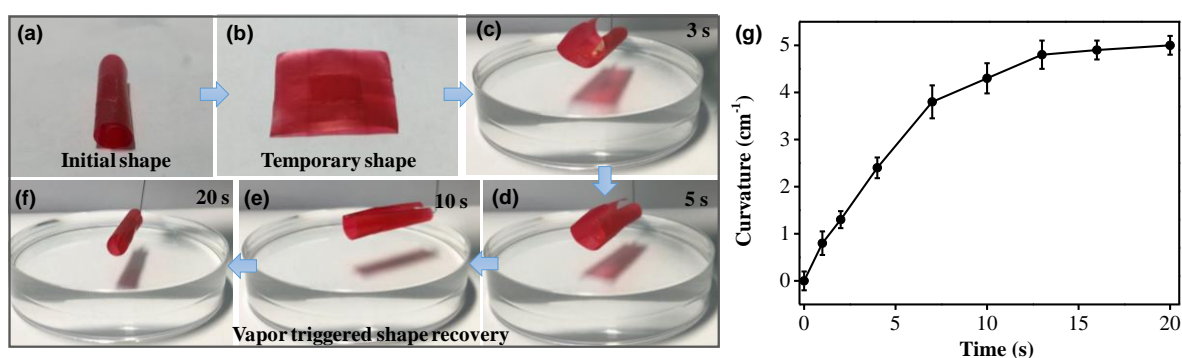


Fig. S11 The water vapor responsive shape memory process (a-f) and the change of curvature with vapor responsive time (g) during shape recovery. The film has curved initial shape (a)

and can fix the unfolded temporary shape after wetting and then drying keeping unfolded state (b). When the surface is moved downward to the hot water ($\sim 80^{\circ}\text{C}$), the film shows fast shape recovery and the curvature increases rapidly. As the time is increased to about 20 s, the film can restore to its initial shape.

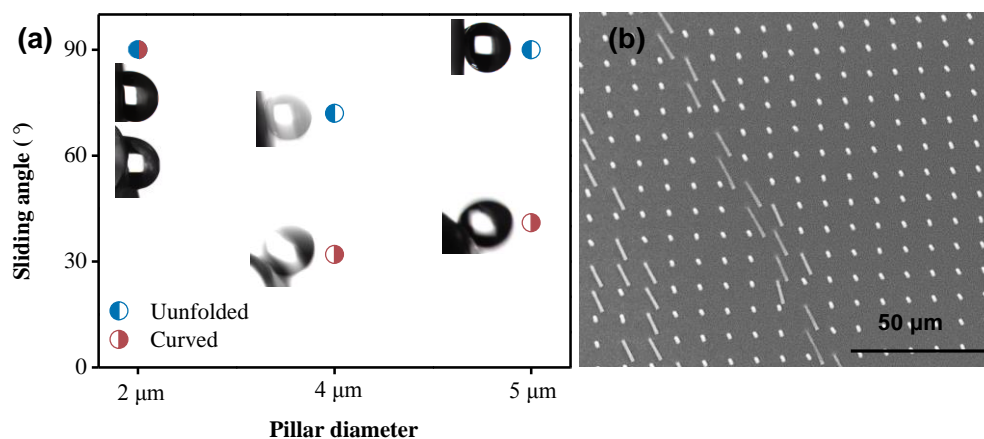


Fig. S12 (a) The variation of the sliding angle with the increase of pillar diameter for film in the curved and unfolded states, respectively. (b) SEM image of the obtained film with pillar diameter of 2 μm.

From Fig. S12, it can be seen that when the pillar diameter is 2 μm, partial collapse of some pillars can be found, and this may be due to the high aspect ratio of pillar that has a poor mechanical stability (b). The water droplet on the surface is hydrophobic high adhesive rather than superhydrophobic in both unfolded and curved states for the film with pillar diameter of 2 μm. When the pillar diameter is 4 μm, the surface can keep superhydrophobicity due to the regular and stable pillar micro-structures, whereas the droplet can roll on the film in both the unfolded and curved states. As the pillar diameter is further increased to 5 μm, the droplet is pinned on the unfolded surface whereas can roll on the

curved surface, showing a good switchable adhesive behavior. Therefore, in this work, the film with pillar diameter of 5 μm was selected for the research of adhesion transition.

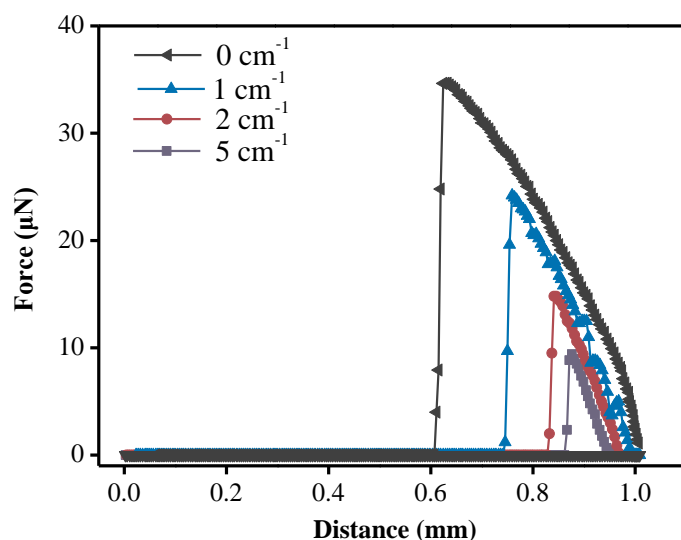


Fig. S13 Force-distance curves for film at different curvatures, indicating that different adhesive forces can be formed on the film with different curvatures, and the surface adhesive force shows decreased trend with the increase in curvature.

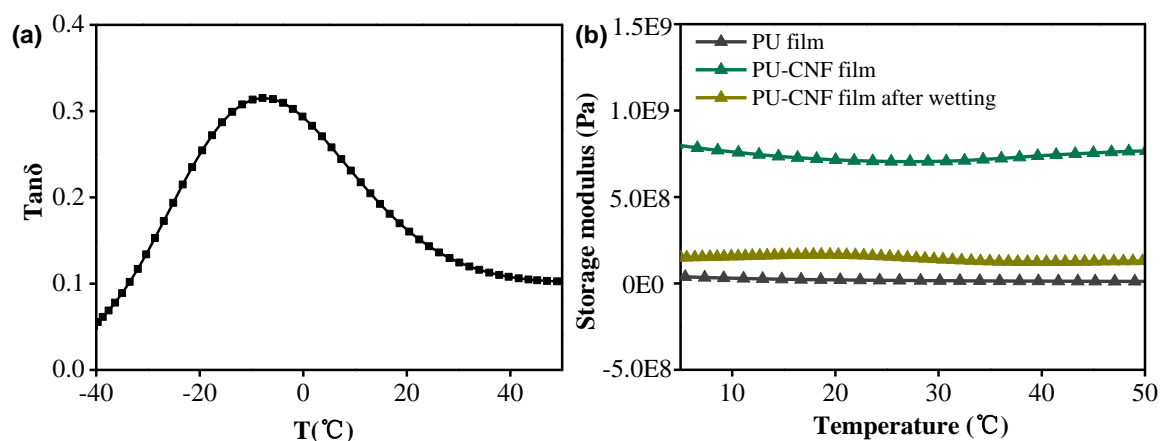


Fig. S14 DMA analysis of pure PU film and the PU-CNF film: (a) the $\tan\delta$ curve vs temperature for PU film, (b) the storage modulus of pure PU film, dried and wetted PU-CNF film, respectively. One can find that the glass transition temperature of PU is about -8°C , indicating that the PU is an elastomer in room temperature. After introduction of CNF, the

modulus is increased apparently for PU-CNF film in both wetted and dried states. Moreover, compared with the wetted state, the PU-CNF film in the dried state has a much higher modulus.

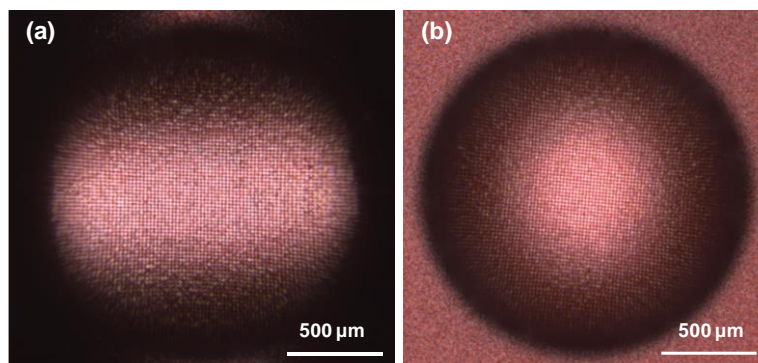


Fig. S15 The confocal microscopy images of s-PU/PU-CNF film under a water droplet at curved state (a) and unfolded state (b), respectively. It can be seen that in both states, lot of air can be found under the droplet (those light area represents the presence of air),^{3,4} indicating the droplet resides in the same Cassie state as the film shape is changed.

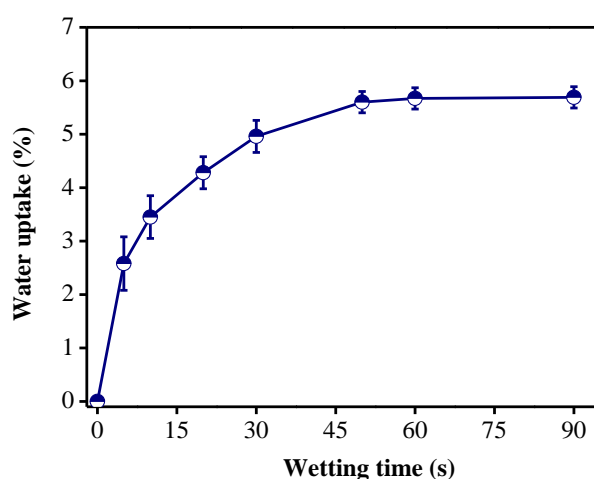


Fig. S16 The variation of water uptake as the increase in wetting time for the film. It can be seen that as the wetting time for the PU-CNF substrate is increased, the adsorbed water is increased. Herein, the water absorb ability of the film were calculated by measuring the samples' weights before and after wetting at room temperature. The weight ratio of water

uptake was calculated according to the following formula: $(m_a - m_b)/m_b$, where m_b and m_a are the weights of the sample before and after wetting by water, respectively.

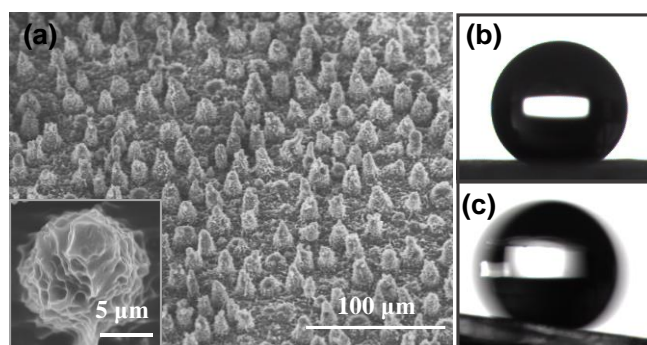


Fig. S17 (a) SEM image of the lotus-leaf-like superhydrophobic PDMS surface after fluoroalkylsilane modification used as the substrate in Fig. 5, which was prepared according to the reference.⁴ (b) and (c) are shapes of a water droplet standing and rolling on the surface, respectively. These results indicate that the prepared PDMS film has a low adhesive superhydrophobicity.

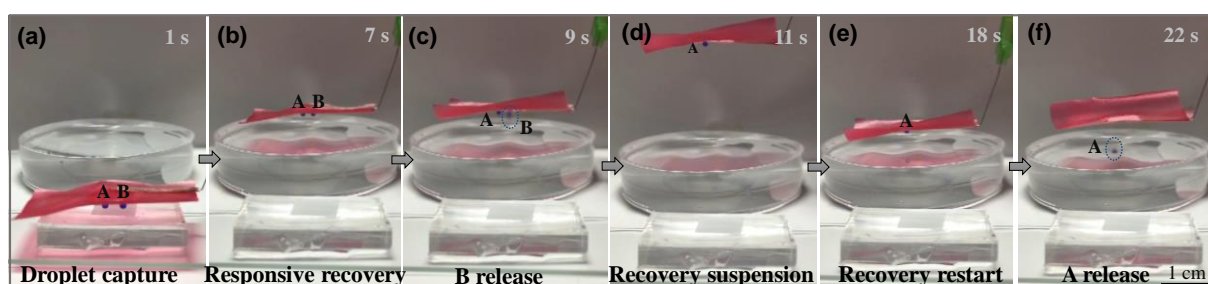


Fig. S18 The controlled release of different microdroplets (movie 3). Two water droplets (A-1.5 μL and B-2 μL) can be first captured by the unfolded temporary high adhesive film (a, b). As the film is put upon the hot water, shape recovery is triggered and the surface adhesive force begins to decrease with the increase of curvature, the large droplet B would firstly be released (c). As the film is lifted, the external stimulus is removed, and as shown in Fig. S18d, the shape recovery process would be suspended, thus the droplet could be stored on the film.

When the film is further closing to hot water (e), the shape recovery is triggered again and the surface adhesive force is decreased further, finally small droplet A would be released (f). The process indicates that controllable release of different droplets can be realized on our film.

Reference

- 1 Y. Z. Wang, Z. J. Cheng, Z. G. Liu, H. J. Kang and Y. Y. Liu, *J. Mater. Chem. B.*, 2018, **6**, 1668-1677.
- 2 C. M. Chen, C. L. Chiang, C. L. Lai, T. Xie and S. Yang, *Adv. Funct. Mater.*, 2013, **23**, 3813-3823.
- 3 J. Gao, Y. Yao, Y. Zhao and L. Jiang, *Small*, 2013, **9**, 2515-2519.
- 4 E. Zhang, Y. Wang, T. Lv, L. Li, Z. Cheng, and Y. Liu, *Nanoscale*, 2015, **7**, 6151-6158.